CrossMark

In situ failure investigation and time-dependent damage test for columnar jointed basalt at the Baihetan left dam foundation

Quan Jiang[1] · Bin Wang[1] · Xia-Ting Feng[1] · Qi-Xiang Fan[2] · Zhilin Wang[2] · Shufeng Pei[1] · Shan Jiang[3]

Abstract

Columnar jointed basalt (CJB), characterized by a hexagonal joint network, poses a great challenge for geotechnical designs due to its time-dependent propensity to deformation and damage. In this paper, the geometrical structure and failure modes of CJB exposed on a dam foundation is presented. The study was conducted during the unloading excavation of the Baihetan dam, China, aiming to provide a more in-depth understanding of the CJB damage mechanism. A systematic field test for the columnar jointed rock mass was also carried out on the dam foundation using ultrasonic P wave measurements. It was found that the excavation damage zone of the CJB not only showed time-dependent damage both in depth and degree but also showed spatially inhomogeneous distribution of the damage degree. Sequential regression analysis further demonstrated the time-dependent behavior of the CJB. Successive observations using digital borehole cameras in the field showed that the unloading damage mechanism of the Baihetan CJB was mainly related to the time-dependent opening of the initially closed joints. Several reinforcing methods for improving the stability of the damaged CJB, including the injection of liquid cement and the installation of the prestressed rock bolts, are discussed.

Introduction

During the intensive excavation of deeply buried tunnels, the joint network inside a rock mass often tends to be loose or open due to the relief of stress, which in turn can often lead to weaknesses in the entire jointed rock mass. The so-called excavation damage zone (EDZ) is often used to describe this excavation-induced deterioration (Maxwell et al. 1998; Brady and Brown 1985; Millard et al. 2009; Zhu et al. 2014) in the form of joint opening and crack propagation (Weinberger et al. 2010; Li et al. 2010; Zhang et al. 2015; Bonilla-Sierra et al. 2015; Pei et al. 2016). The damage to the jointed rock mass during the unloading process often

causes serious problems. The largely reduced modulus of a damaged rock mass leads to inhomogeneous settlement and subsequent deformation of the installed upper structures (Ozcan et al. 2013; Xiang et al. 2015; Kofichko 1996; Justo et al. 2014). Additionally, unloading of the confining stress generally leads to shearing deformation and slipping failure of the whole joint, resulting in collapse or sliding of the jointed rock mass (Sharifzadeh et al. 2010; Maleki 2011; Satıcıo and Unver 2015; Jin et al. 2015).

The actual damage to the jointed rock mass is a process of dynamic evolution that starts under a certain initial geo-stress state (σ_1, σ_2, σ_3) during excavation-associated unloading. It develops with time and slows down at a certain redistributed stress state after excavation. The in situ test provides a key tool to understand the real damage behavior of jointed rock masses, because no laboratory experiments can reproduce the actual geo-stress conditions and the complex in situ engineering boundaries (Watters et al. 2000; Gage et al. 2014; Yarahmadi et al. 2015; Zhan et al. 2016). Many in situ testing methods have been proposed to evaluate damaged rock masses, such as ultrasonic wave testing, borehole camera/television, and micro-seismic monitoring. Meaningful findings on rock mass damage have been reported, such as the opening of

✉ Bin Wang
  bwang@whrsm.ac.cn

1 State Key Laboratory of Geomechanics and Geotechnical Engineering, Institute of Rock and Soil Mechanics, Chinese Academy of Sciences, Wuhan 430071, China

2 China Three Gorges Project Corporation, Beijing 100038, China

3 Department of Mechanical Engineering, University of Mississippi, Oxford, MS 38677, USA

existing joints, the generation of new cracks, and the intersections of fractures (Li et al. 2013; Rodriguez et al. 2014; Armand et al. 2014; Scholtès and Donzé 2015). Field and laboratory evidence has shown that damage of a jointed rock mass is a time-dependent behavior due to joint opening, closing and extension (Malan 2002; Fahimifar and Soroush 2005; Shao et al. 2006; Li et al. 2011). However, the available field test data obtained so far about the time-dependent performance of the jointed rock mass EDZ are insufficient. Thus, insufficient data restrict the engineering estimations of jointed rock mass damage in practice and leads to many uncertainties in long-term safety engineering of dam foundations (Nabil and Ala 2001; El-Naqaand Kuisi, 2002; Lin et al. 2015; Fan et al. 2015).

As a typical example of an embedded joint rock mass, the columnar jointed rock mass presents a "special" geological structure. The joint network formed in an ordered colonnade pattern consists of roughly hexagonal units, and is transversely cut by other joint sets (Schultz 1995; Lore et al. 2000; Jiang et al. 2014). Some typical columnar jointed rock sites, such as the Chinese Tengchong, Hong Kong's High Island Reservoir, and the US Banks Lake, have now become popular landscape attractions for their unique beauty (Lucas and Stephen 2008; Fang et al. 2011), as shown in Fig. 1. It is widely accepted that columnar jointed rock masses originate from lava flows and are formed by thermally induced contraction–cooling (Lore et al. 2000; Budkewitsch and Robin 1994; Müller 1998; Goehring et al. 2006). However, their geotechnical engineering response to unloading excavation has rarely been discussed due to limited engineering practice. The exposed columnar jointed basalt (CJB) at the Baihetan hydropower station in southwest China is a typical columnar jointed rock mass. Due to its undesirable geotechnical properties, such as the jointed structure, brings challenges to the construction of the concrete dam and underground tunnels. Prior

investigations and tests have shown that the CJB has a low deformation modulus and strength and thus results in heterogeneous settlement and slope instability for the dam (Yan et al. 2011; Shan and Di 2013; Feng et al. 2016; Zhang et al. 2016). According to the corresponding Chinese national standards, engineering experiences and the Baihetan hydraulic design standards, the classification of the rock mass quality on the dam foundation after excavation must satisfy the "III" rank, and its ideal deformation modulus should be larger than 6 GPa (El-Naqa and Kuisi 2002; PSCC 2003; PSCC 2005; Shi et al. 2008; Wu et al. 2009a; Luo et al. 2015). Therefore, detailed field tests on the depth and corresponding time-dependent evolution of the EDZ are essential for the safety assessment of the concrete dam. In addition, understanding the time-dependent mechanical properties of the CJB after excavation is of great importance for making a timely decision to reinforce the CJB in the dam foundation, such as the installation of rock bolts, anchor cables, grouting, etc.

In the present work, we carried out a detailed investigation of the geometric characteristics and the unloading-induced failure performance of the CJB on the left side of the Baihetan dam base. The field test data were obtained from the ultrasonic wave detection of 30 boreholes in the columnar jointed rock mass. The evolution of the entire damaged depth after excavation, the spatial distribution and time-dependent evolution of the damage degree in the EDZ were also studied using back statistical analyses. The CJB damage mechanism was investigated with the aid of additional field observations by using a digital borehole camera. Reinforcement measurements for the damaged CJB on the Baihetan dam base are then discussed according to the reported field test results.

Background of the Baihetan project

The Baihetan hydropower station is located on the lower reaches of the Jinsha River, China, with its left bank on the side of Ningnan County in Sichuan Province and its right bank on the side of Qiaojia County in Yunan Province. The station, with a total of 1600 MW of installed capacity, is the second largest hydraulic project in China (only smaller than the Three Gorges station). Its concrete dam, designed as a double-curvature arch format, is situated in an unsymmetrical V-shaped valley. The arch dam is 289 m in height, with the crest at 834 m asl, and the normal reservoir water level is at 825 m, as shown in Fig. 2a. Igneous basalt in the Baihetan region is the result of historic magmatic and volcanic eruptions. The rock stratum is typically a monoclinal orientation, with the geological attitude of NE30°–50° in trend and SE∠15°–25° in dip angle. The surface weathering of the rock mass in the dam's valley is evident. The horizontal weathering depth on the left bank is approximately 67–89 m, and pm the right bank it is relatively smaller, possibly approximately 29–45 m due to

Fig. 1 Typical scenic spot of the columnar jointed rock mass at the Washington Banks lake
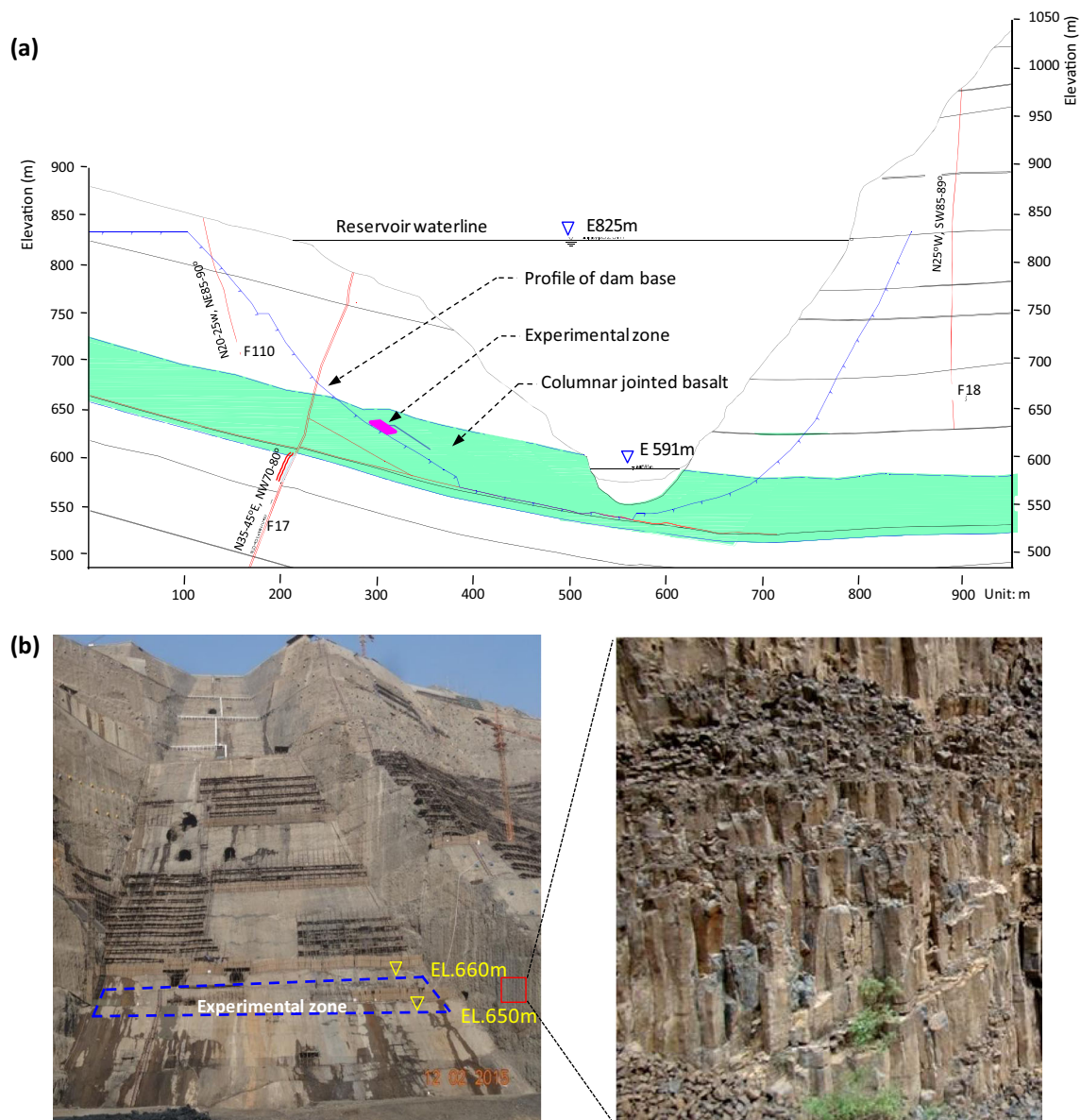
(Luacs and Stephen, 2008)

Fig. 2 The Baihetan dam foundation: (a) typical geologic transverse profile of the valley; (b) exposed columnar jointed basalt on the left dam site

the non-uniform unloading effects on the left and right banks. The field measurement of the initial geo-stress ranges from 4.89 to 10.0 MPa in the valley region, whereas under the river bottom, the maximum principal stress can reach approximately 40.32 MPa.

The basalt on the dam site belongs to the upper Permian system ($P_2\beta_4{}^2$–$P_2\beta_3{}^3$), and the typical CJB exposed on the dam base ranges from 575 to 670 m in altitude on the left bank and from 585 to 545 m on the right bank (Fig. 2b). The CJB, characterized by small columnar blocks, formed the cooling process of the lava from a volcanic eruption in the Permian epoch. The CJB prisms on the left bank are irregular polygons in cross-section, and the axis trends towards the valley with a dip angle of approximately 70°. Prior tentative field tests, such as the in situ triaxial compression tests and the

bearing plate test in some experimental tunnels at other positions (Jin et al. 2015), showed that the deformation modulus of the undisturbed CJB approximately ranged from 7 to 11 GPa along the horizontal direction, and from 5 to 9 GPa in the vertical direction. However, after the excavation, the deformation modulus test by bearing plate experiment sharply decreased to a lower range of 3.0–5.2 GPa along the unloading direction due to the induced excavation damage (Shi et al. 2008;Justo et al. 2006; Xu et al. 2011, Cui et al. 2018).

Overall, both the structural strength and the deformation modulus investigation for the CJB indicated the seriously excavation-induced deterioration on the dam base. Hence, the structural characteristics and the time-dependent damage of CJB are key factors for the general stability of the concrete dam and the long-term safety of the reservoir. Therefore, an

experimental zone was selected at an altitude of 650–660 m, as shown in Fig. 2b, for a more detailed investigation of the CJB structure and its time-dependent damage behavior after excavation.

## Investigation for filed CJB on the dam base

Along with the excavation of the rock mass above the dam base, an in situ investigation was carried out at the altitude of 620–670 m where the CJB was exposed. The geological analysis showed that the CJB mass was cut by three types of joint sets with different physical properties and geometric scales, i.e., a columnar joint set between prisms at the meter scale, an upright internal joint set inside the prism at the decimeter scale, and a horizontal internal joint set inside the prism at the centimeter scale, as shown in Fig. 3. These joint sets consisted of a complicated joint network that deeply affected the mechanical properties of the CJB. The equivalent cylindrical diameter of the columnar blocks and the average space of the horizontal joint sets were key parameters for understanding the whole geometric structure of the CJB.

Geometric statistical analysis for field CJB

It has been shown that the exposed prism sections of the CJB on the dam foundation were not only of hexagonal shape but also of other kinds of irregular polygons because of the unsatisfactory historical heat-exchange environment (Saliba and Jagla 2003; Bosshard et al. 2012; Hetenyi et al. 2012). Moreover, the prismoid axes were not vertical due to the inclined stratum. The scanline mapping technique and the stereographic projection method were therefore utilized to investigate the geometric characteristics of the CJB.

The excavated surface of the dam foundation and the walls of the surveying tunnels inside the CJB were the available measuring windows. Considering the complicated close joint structure, a reasonable choice of measuring lines was very important. Three groups of measuring lines in trends 10°, 65°, and 126° were selected, intersecting roughly at 60° to each other, as shown in Fig. 4a. Moreover, this layout can also avoid the possible orientation dependency of the measuring lines. Therefore, the edge lengths of the exposed prisms along the measuring lines and the orientations of columnar joints on the surface can be measured. Along these measuring lines, the

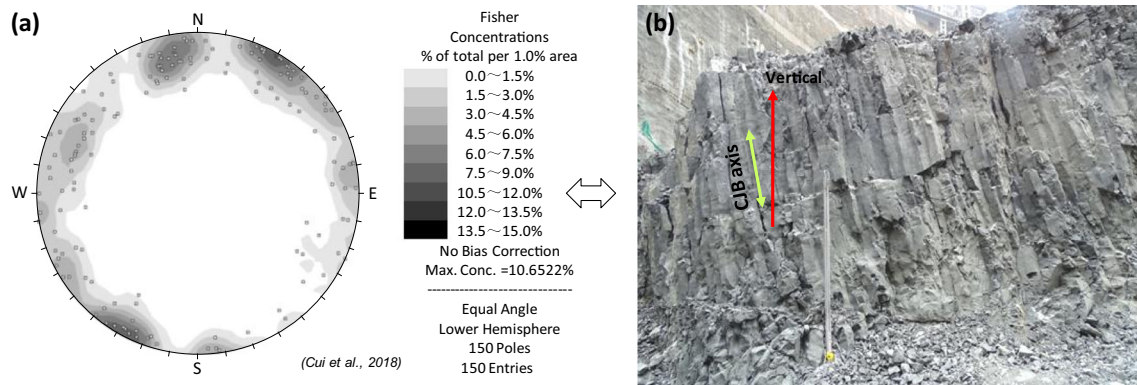**Fig. 3** CJB's joint network including three types of joint sets
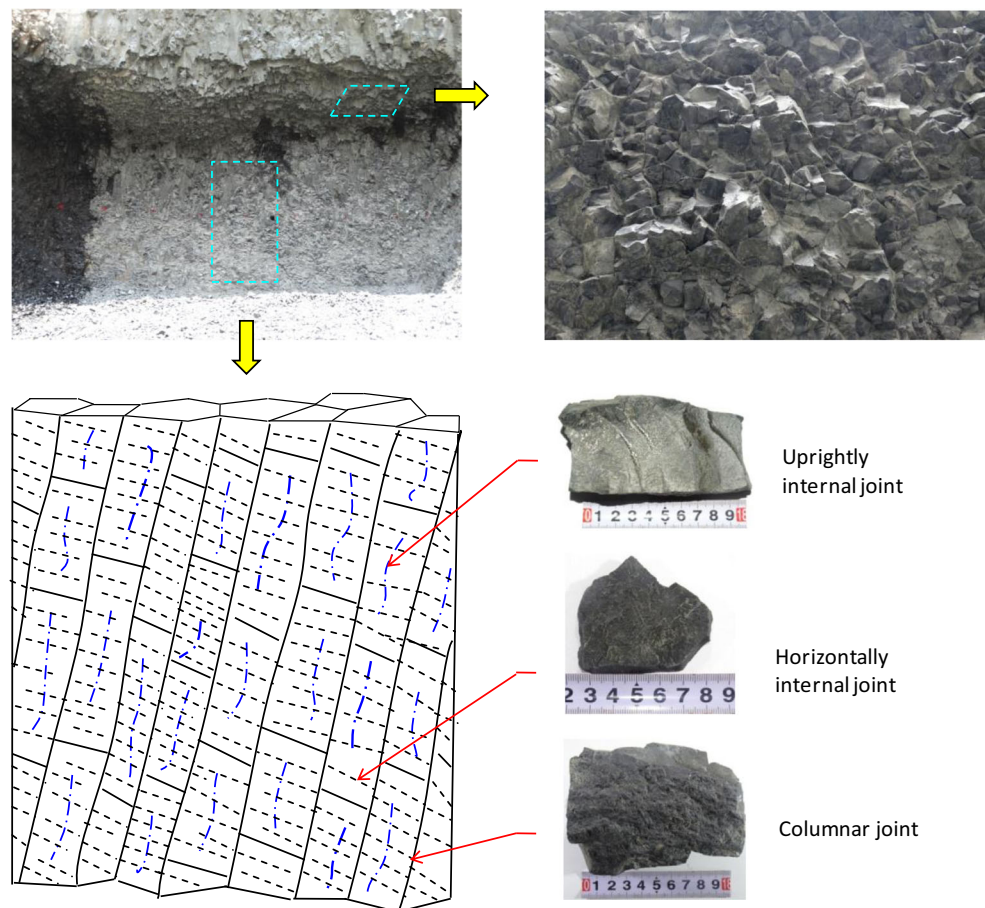
Fig. 4 Poles contour diagram of columnar joints (**a**) and field CJB exposed on the slope (**b**)

columnar joint orientations can be obtained. To ensure an objective and reasonable statistical result, a total of 150 sets of altitude parameters of the joints in three groups (50 sets for each group) were measured randomly. All these joint orientation data were analyzed with Schmidt pole plots and contour diagrams (see Fig. 4a). In the Schmidt net diagram, the pole plots were shown to be nonsymmetrical, which directly proved that the CJB cross-section was an irregular polygon. This result was in good agreement with the field observations, as shown in Fig. 4b. In addition, the pole plots in the diagram were not lumped in certain localized zones, and were not similar to those of a regular stratified rock mass. This implied that the columnar joints had a special closed intersection network pattern as well as the same dip angles to a large degree.

The investigation of the transverse sections of the CJB exposed on the surface showed that most of the block sections were quadrangular and pentagonal due to the intensive incisions from the steep joint network, as shown in Fig. 5. Measurements on the diameter of the columnar blocks in the exposed CJB on the dam foundation showed that the block edges were 15–35 cm in length, with an average of 29 cm (Table 1), based on 190 samples. Moreover, the logarithmic normal distribution reasonably described the variability of the CJB edge lengths.

Figure 6 showed the frequency histograms of the intervals and the fitted lognormal frequency function of the horizontal joint set inside the columnar blocks. The lognormal distribution fitted the observed results reasonably well, showing the mean value of 1.36 cm. This kind of joint set originated from the delayed cooling of the lava as mentioned above and was initially closed before the excavation due to the surrounding high geo-stress. When the upper rock mass was excavated, the normal stress on the joint plane experienced an unloading process. Hence, this intensively horizontal joint set exposed on the dam foundation was loosened and partially opened step by step, thereby leading to the decrease in the deformation modulus with time. This process should also cause time-

dependent deformation and local failure of the rock mass due to the reduced frictional forces on the joint plane.

Field failures of the CJB on the dam foundation

The field investigation showed that this exposed columnar jointed rock mass exhibited several types of failure modes, including opening of columnar prisms, cracking of concrete, loosening of internal joints, and shearing deformation of horizontal joints (Fig. 7). These kinds of failure may all be related to the CJB joint sets.

1) The opening of the columnar and vertical internal joint sets induced in the separation of columnar prisms, as well as the disintegration of the columnar block itself, as shown in Fig. 7a. These local deformations of columnar prisms may easily lead to the cracking of sprayed concrete on the dam base (see Fig. 7b).
2) The opening of horizontal internal joint sets easily resulted in the shearing tendency of the columnar blocks, as shown in Fig. 7c. This type of opening may also cause extra shearing deformation and even local collapse due to the reduced frictional resistance if no appropriate supporting measurements were applied, as shown in Fig. 7d.

Time-dependent damage tests for the CJB

To understand the unloading damage response of the CJB on the left dam foundation after excavation, we selected a rectangular experimental zone of 90 m in length and 14 m in height on the dam base to consider the field testing condition, as shown in Figs. 2a and 8. A series of tests were carried out to study the time-dependent CJB damage behavior using ultrasonic P wave methods.
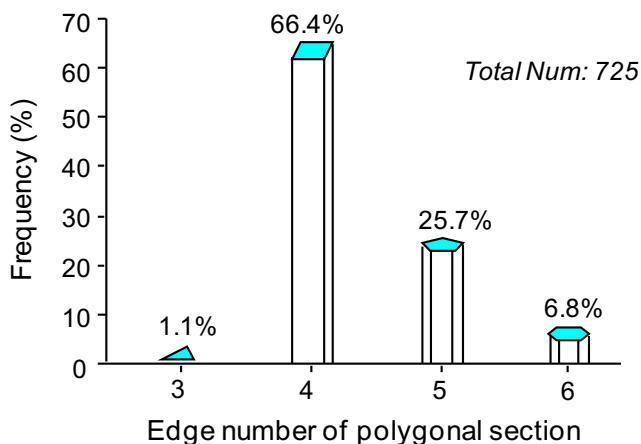
Fig. 5 Statistical polygon ratio of the CJB transverse section

Testing scheme

The experimental zone was entirely in the columnar jointed rock mass, and its surface was inclined to the Jinsha River with a dip angle of approximately 45°. A shearing belt with a small dip angle (approximately 15°–25°), called LS3319, ran through the testing zone and introduced differences of rock mass quality. The quality classification of the CJB mass below the shearing belt was III-1 rank, whereas the CJB quality classification above was slightly weaker, i.e., III-2, according to the Chinese national standard for engineering classification of rock masses (DB 50218 1995; Chen and Xu 2017). The experimental zone was divided into three subzones, i.e., the downside region of LS3319, subzone A; the upper region of LS3319 at EL 660–655 m, subzone B and subzone C, as shown in Fig. 8. Thus, these geological differences between subzones might affect the initial damage depth induced by the unloading excavation for the dam foundation.

Thirty boreholes in total were drilled in the experimental zone before the excavation, with each experimental subzone including 10 boreholes. All these testing holes were normal to the face of the experimental zone and were 10 m in length. The test used the ultrasonic P wave detection method in a single borehole (Aydin 2014; Meglis et al. 2005), and the detection probe had one emission component and two receiving components (Fig. 9). For every 0.1 m as the probe moved in the borehole along the axes, a P wave velocity data would be obtained. And, by assembling all the data, a wave–velocity curve along the borehole depth could be obtained (Aydin 2014; Malmgren et al. 2007; Wu et al. 2009b). By evaluating the tested curves, the damage depth of the Baihetan CJB was defined as the point at the obvious turning point on each curve.

If there was no obvious turning point, a point with a 10% reduction in the wave velocity in the undamaged segment would be used.

The wave velocity of the undisturbed columnar jointed rock mass was obtained from Eq. (1). The average P wave velocity of the undamaged rock mass in testing holes was defined as:

$$\overline{v^o} = \frac{1}{n} \sum_{i=1}^{n} v_i^o \qquad (1)$$

where $\overline{v^o}$ is the average P wave velocity of the undisturbed columnar jointed rock mass, v_i^o is the measured P wave velocity of the non-damaged parts along the borehole, and n is the number of measured velocities.

Temporal evolution of the CJB damage depth

The field testing of the CJB experimental zone lasted for 7 months. All the detected curves of P wave velocity versus depth for the boreholes showed that the lower P wave velocity appeared at the shallower part and the higher P wave velocity appeared at the deeper part (i.e., undisturbed rock mass) in the borehole, as shown in Fig. 10. These results indicated that both the final stable damage depth and the EDZ stable time were different in different subzones; for example, the average CJB damage depth at subzone A was smaller than subzones B and C, as shown in Fig. 11.

All the testing work began in Novrmbrt 2014, the day after the upper rock mass above the experimental zone was excavated by blast. In situ tests by the ultrasonic P wave apparatus showed that:

1) The average P wave velocity of the undisturbed CJB was approximately 5132 m/s, but that of the damaged columnar jointed rock mass was in the range of 4800–3200 m/s in subzone A. The final depth of the EDZ stabilized within less than 15 days; whereas the adjacent blasting opening could induce a sharp depth increase that could be observed in boreholes A1–5 and A2–1, as shown in Fig. 12.

2) In subzone B, the average P wave velocity of the undisturbed CJB was approximately 5072 m/s, but that of the damaged columnar jointed rock mass was in the range of 4700–2960 m/s. It was evident in Fig. 13 that the CJB in subzone B had time-dependent damage behavior, as the damage depth increased with time continuously, until

Table 1 Statistical data of edge length for the columnar jointed blocks	Random parameters	No. sample	Min. length	Max. length	Ave. length	SD	Optimal probability distribution
	Value	190	12 cm	64 cm	29 cm	7.9 cm	Logarithmic normal

**Fig. 6** Statistical interval distribution of the horizontal joint set
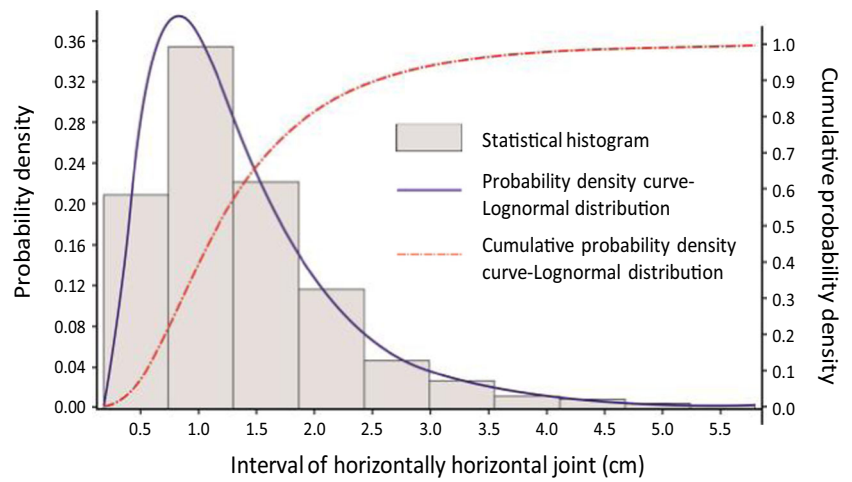
approximately 30 to 45 days after the excavation. Then, the EDZ depth finally stabilized.

3) The average P wave velocity of the undisturbed CJB was approximately 5085 m/s in subzone C, but that of the damaged columnar jointed rock mass was in the range of 4600–2890 m/s. The CJB at subzone C also obviously had time-dependent damage behavior, as shown in Fig. 14. Consistent with the findings in subzone B, it took approximately 3045 days for the EDZ depth evolution to stop.

Fig. 7 Field failure performances of columnar jointed basalt exposed on the dam foundation: (**a**) opening of columnar prisms, (**b**) cracking of concrete, (**c**) loosening of internal joint, (**d**) shearing deformation of horizontal joint
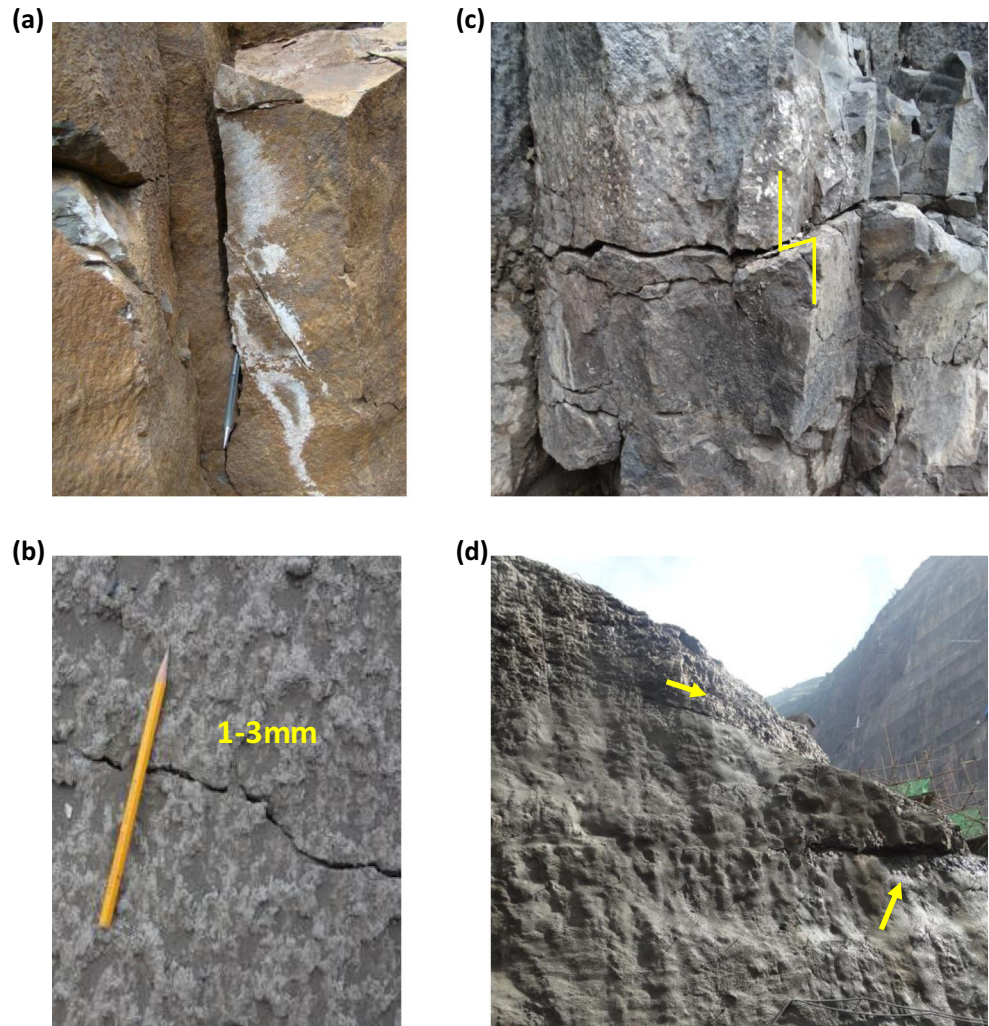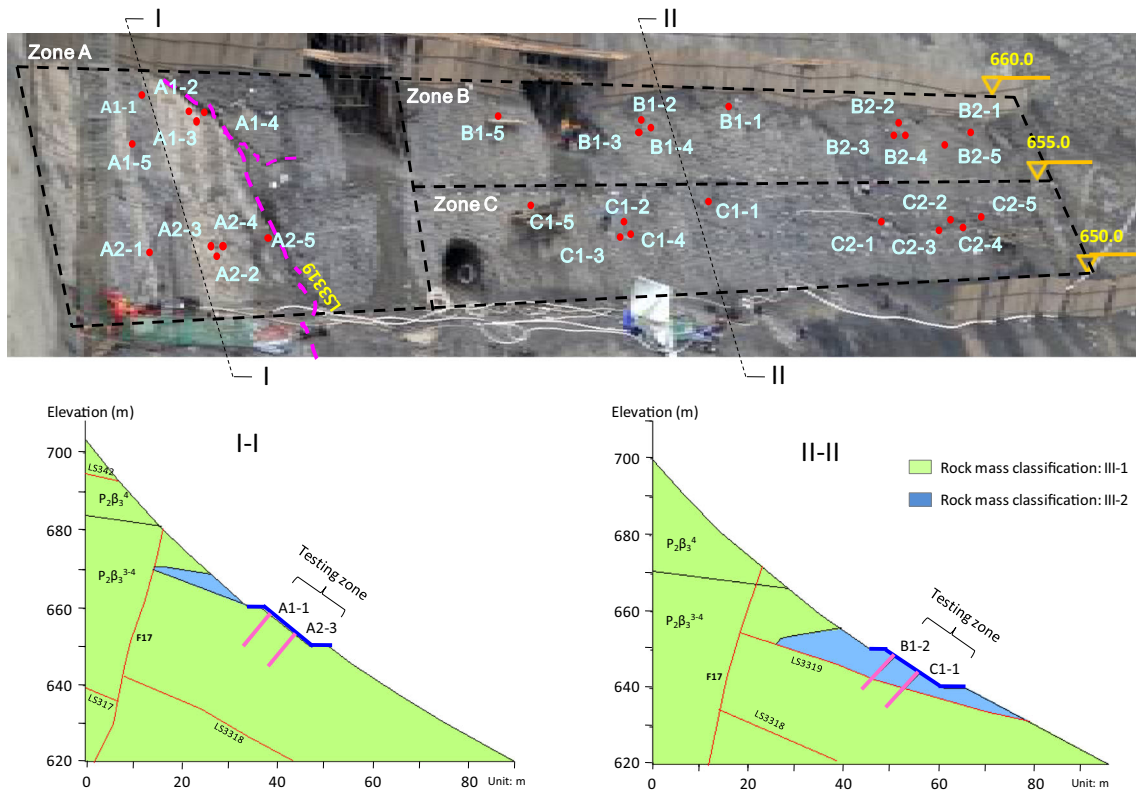
Fig. 8 In situ experiment site and corresponding subzones

By comparing Figs. 12, 13 and 14, it can be found that the time-dependent CJB damage in subzones B and C was more serious than in subzone A, although all the temporal damage ceased after a long time, as recorded in Table 2. The differences of the tested results between the subzones maybe related to the rock quality and influenced by the shearing belt, i.e., LS3319, in the experimental zone.

To obtain the temporal evolution pattern for this III-2 rank columnar jointed rock mass, regressive analyses were

Fig. 9 The integrated ultrasonic wave detection equipment for rock damage

performed based on the damage depth data obtained in subzones B and C. The results showed that the temporal evolution of the CJB damage depth was generally in accordance with the Curtis logic equation (Eq. 2),

$$L = \frac{1}{1 + 3.6064\, e^{-0.1144T}} \qquad (2)$$

where L is the normalized EDZ damage depth ratio, i.e., the current/final damage depth, and T is the time of the CJB after excavation. Figure 15 shows the obtained data and the fitted Curtis curve, and the results match each other reasonably well. It is also worth noting that as T became sufficiently long, the damage depth ratio L would converge to a constant, given that there was no external disturbance.

Spatial damage degree in the EDZ of the CJB

The in situ detections shown above revealed that the P wave velocities in the EDZ of the CJB varied at different depths of the borehole. This was manifested by the fact that low velocity was detected at the shallower part and high velocity was detected at the interior part along the borehole axis (Fig. 16). The result indicated that the damage degree of the unloaded CJB EDZ was spatially inhomogeneous, which may also leaded to spatial anisotropy of the CJB deformation modulus.

Fig. 10 Typical tested P wave velocity vs. depth cures in the boreholes (tested at 15 days after excavation)
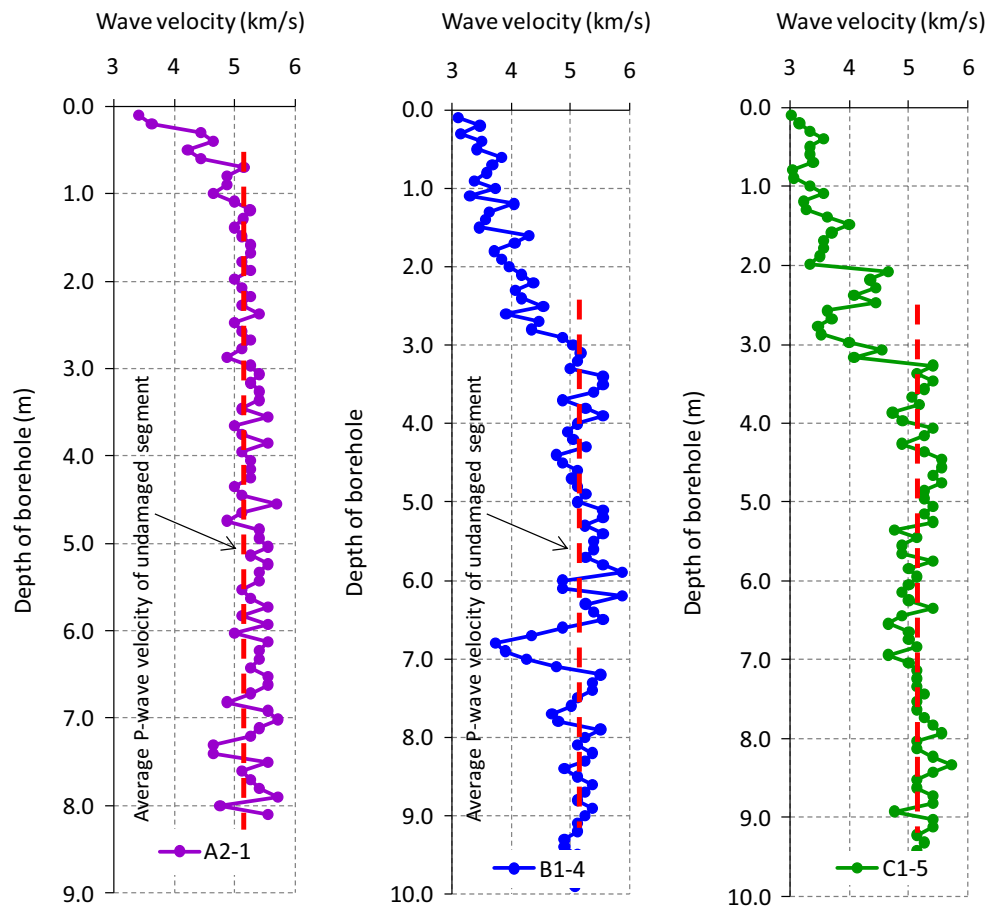
According to Rabtonov's 1963 definition of the damage index for a destructive test (Rabtonov 1963), the damage of the rock mass can be defined by the wave velocity,

$$D_f = 1 - {v_i}/{v^o} \qquad (3)$$

where D_f refers to the damage degree of the rock mass. The damage degrees of the CJB's EDZ in subzones B and C were thereby calculated, and the results clearly showed

heterogeneous damage after excavation. As shown in Fig. 17, serious damage occurred at the opening of the hole, whereas no or little damage was found in the deeply undisturbed rock mass. Regression analyses were carried out based on the damage data of the B and C subzones, and the results indicated the Sigmoid function can ideally describe the spatial distribution of spatial damage degree for the Baihetan columnar jointed rock mass from the surface to the interior. It is shown in terms of Eqs. 4 and 5,
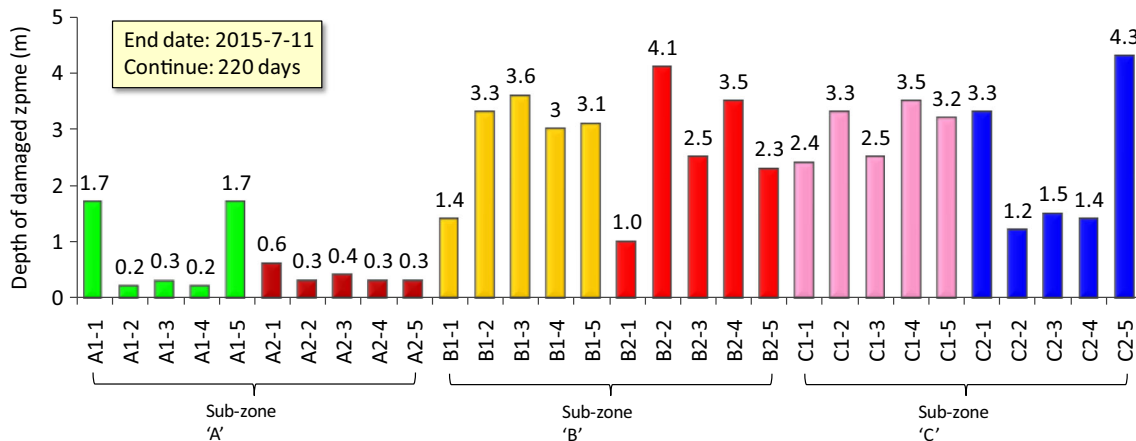

Fig. 11 Total tested depths of EDZ in the CJB experimental zone (results at 220 days after excavation)
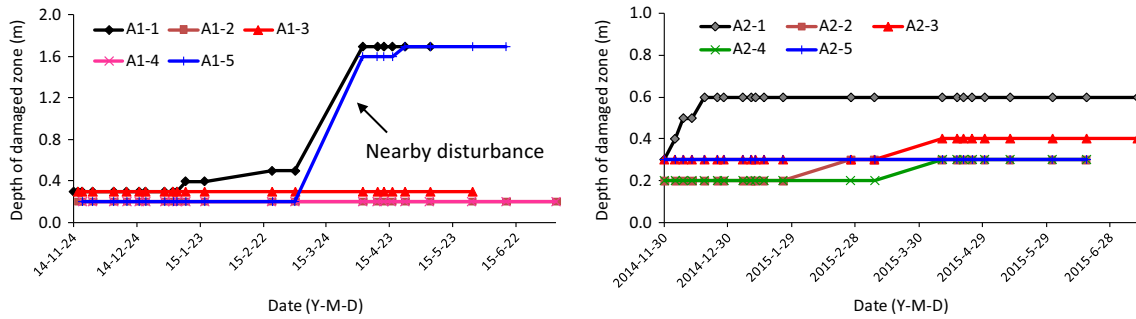
Fig. 12 Temporal evolution of the CJB damage depth gained in subzone A

$$D_B^{mid} = 1 - \frac{1}{1 + 2.7197e^{(1-3.3456P)}}$$

$$D_B^{down} = 1 - \frac{1}{1 + 1.0879e^{(1-3.3456P)}} \qquad (4)$$

$$D_B^{up} = 1 - \frac{1}{1 + 6.7993e^{(1-3.3456P)}}$$

$$D_C^{mid} = 1 - \frac{1}{1 + 3.1197e^{(1-3.5658P)}}$$

$$D_C^{down} = 1 - \frac{1}{1 + 1.2479e^{(1-3.5658P)}} \qquad (5)$$

$$D_C^{up} = 1 - \frac{1}{1 + 7.7993e^{(1-3.5658P)}}$$

where P is the ratio between the current testing position and the final EDZ depth; D_B^{mid}, D_B^{up}, and D_B^{down} are the middle fitting, up boundary, and down boundary equations for testing in subzone B, respectively; and D_C^{mid}, D_C^{up}, and D_C^{down} are the middle fitting, up boundary, and down boundary equations for testing in subzone C, respectively.

Time-dependent damage evolutionof CJB's EDZ

Since the disturbed CJB showed spatially inhomogeneous damage degree characteristics, the time-dependent evolution of the CJB at different positions was further analyzed. P wave velocity data with a final damage depth of more than 2 m in subzones B and C were selected and analyzed. The velocity data in the EDZ were divided

uniformly into 5 segments along the borehole axis, i.e., 0–1/5, 1/5–2/5, 2/5–3/5, 3/5–4/5, and 4/5–1 of EDZ depth. The average velocity for the testing data of a given depth at different testing times was calculated. Figure 18 summarizes the computed results for each segment, as well as the fitting functions. It was shown that the average velocity of all the testing data had a tendency of time-dependent reduction, although the fitting function and final stable values were different. It was also shown that the time-dependent decrease of the CJB velocity in the EDZ was self-convergent under no disturbance (i.e., converging to a constant value).

Regression analyses for the above velocity data in different depths showed that the negative exponent function, as described in Eq. 6, can reasonably describe the time-dependent evolution of CJB velocity,

$$D(t) = a \cdot t^{-b} \qquad (6)$$

where D is the damage degree, t is the time, and a and b are the fitting parameters corresponding to different positions. It was interesting to note that none of the fitting curves cross into each other, as shown in Fig. 18f. By converting the weakening degree in the P wave velocity into the damage degree according to Eq. 3, it can be found that the time-dependent evolution of the damage degree in the CJB seems to have a similar deteriorating pattern in different positions.

In summary, the field observations from the ultrasonic P wave velocity tests indicate that the EDZ of the CJB on the
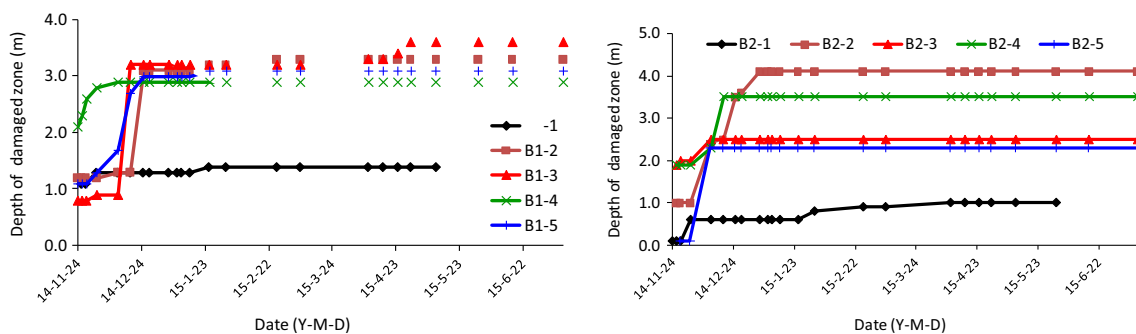

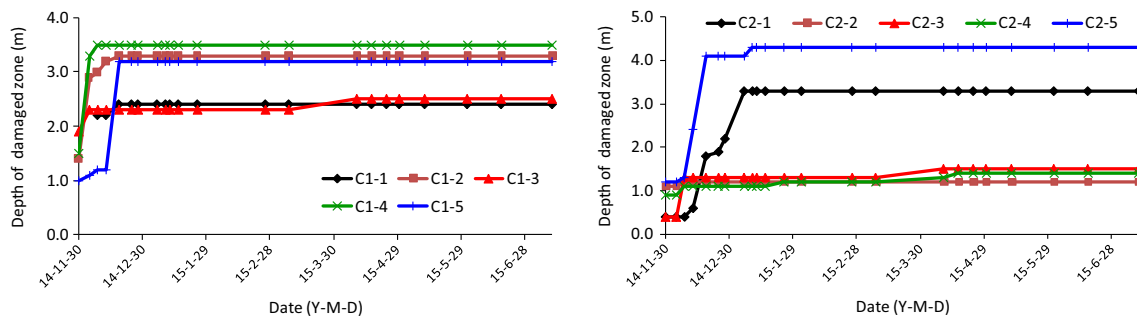Fig. 13 Temporal evolution of the CJB damage depth gained in subzone B

Fig. 14 Temporal evolution of the CJB damage depth gained in subzone C

dam foundation experiences not only spatially inhomogeneous damage in degree but also temporal damage in depth and degree. Therefore, the EDZ of the Baihetan columnar jointed basalt can be considered as a 4D damage process, i.e., having spatially 3D inhomogeneous deformation and time-dependent evolution.

Discussion

Generally, the jointed rock mass is composed of intact rock and joint sets (Barton et al. 1974; Hoek and Brown 1997; Sakurai 2010), and, hence, its damage mechanism should be distinguished from normal homogeneous material. To grasp the damage principle of the columnar jointed rock mass, a digital borehole camera (DBC) was used to observe the unloading damage behavior of the CJB in the testing holes. The results showed that many open joints existed in the testing borehole, with widths of 0.1–3 mm, as shown in Fig. 19. Through successive surveys by the DBC, it was also shown that joint widths gradually changed with time. Due to the excavation, the stress within the surrounding rock mass was unloaded, initiating the opening of the originally closed joints. However, until a new mechanical equilibrium state was reached, the induced open of joints developed continuously. Meanwhile, the mechanical properties of the damaged CJB, such as the deformation module, shearing strength, wave velocity, etc., became weakened.

Since opening of the joints inside the CJB was the intrinsic mechanism of time-dependent damage and a

key factor for the stability of dam construction, the necessary technical means must be carried out to reduce or close up the joints, and improve CJB mechanical properties. Assuming the opening of the original joints was following the principal CJB damage mechanism, the damage degree can also be defined by its geometric definition (Kachanov 1958), i.e.,

$$D = 1 - \overline{A}/A_0 \qquad (7)$$

where D is the material damage degree, A_0 is the initial cross-sectional area of the undamaged material, and $\overline{A}$ is the effective loading area of the damaged material. By comparing with Eq. (3), where the damage degree is defined by the wave, the rock wave velocity can be considered directly proportional to the effective loading area in the excavated damage zone, i.e.,

$$v_i \propto \overline{A} \qquad (8)$$

Therefore, the rehabilitation of the damaged CJB can be achieved by increasing the effective contacting and loading area of the rock mass.

In addition, as a typical friction-type material, the rock mass strength generally satisfies the Mohr–Coulomb criterion, i.e.,

$$\tau = C_0 + \sigma_n \tan\varphi \qquad (9)$$

where τ is the material shearing strength, C_0 is the cohesion, σ_n is the normal stress, and φ is the friction angle. To improve

Table 2 Summarization of damage characters for the CJB in different zones

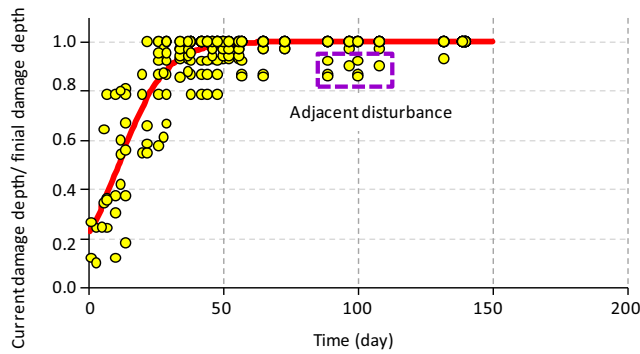| Testing position	Start time	Testing time	Wave velocity of EDZ (m/s)	Ave. wave velocity of undisturbed CJB(m/s)	Temporal evolution duration
Sub-zone A	Nov. 2014, 1 day after excavation	7 months	4800–3200	5132	Less than 15 days
Sub-zone B			4700–2960	5072	About 30–45 days
Sub-zone C			4600–2890	5085	About 30–45 days

Fig. 15 Fitting curve of Curtis logic equation for the damage depth data gained in the subzones B and C

the effective loading strength of the damaged jointed rock mass, one way is to amend the physical properties of the material (C_0 and φ), and the other way is to enhance the

exterior normal stress (σ_n). Therefore, two technical methods can be employed:

1) Perform the injection of liquid cement inside the damaged rock mass, which can solidify the joints and fill their lacunas, i.e. to increase the effective loading area, and also improve the C_0 and φ of the CJB;

2) Install prestressed rock bolts to enhance the normal stress on joints and restrain further cracking of the CJB.

During the actual reinforcement of the columnar jointed basalt on the dam foundation, wet-ground cement with 0.5 MPa pressure was grouted inside the columnar jointed rock mass and rock bolts with 120 kN prestress were also installed to limit the time-dependent deformation and damage (Fig. 20). The corresponding DBC test indicated that these methods can improve the integrity of the columnar jointed basalt.

Fig. 16 Typically time-dependent reduction of P wave velocity curve and increase of damage depth in EDZ
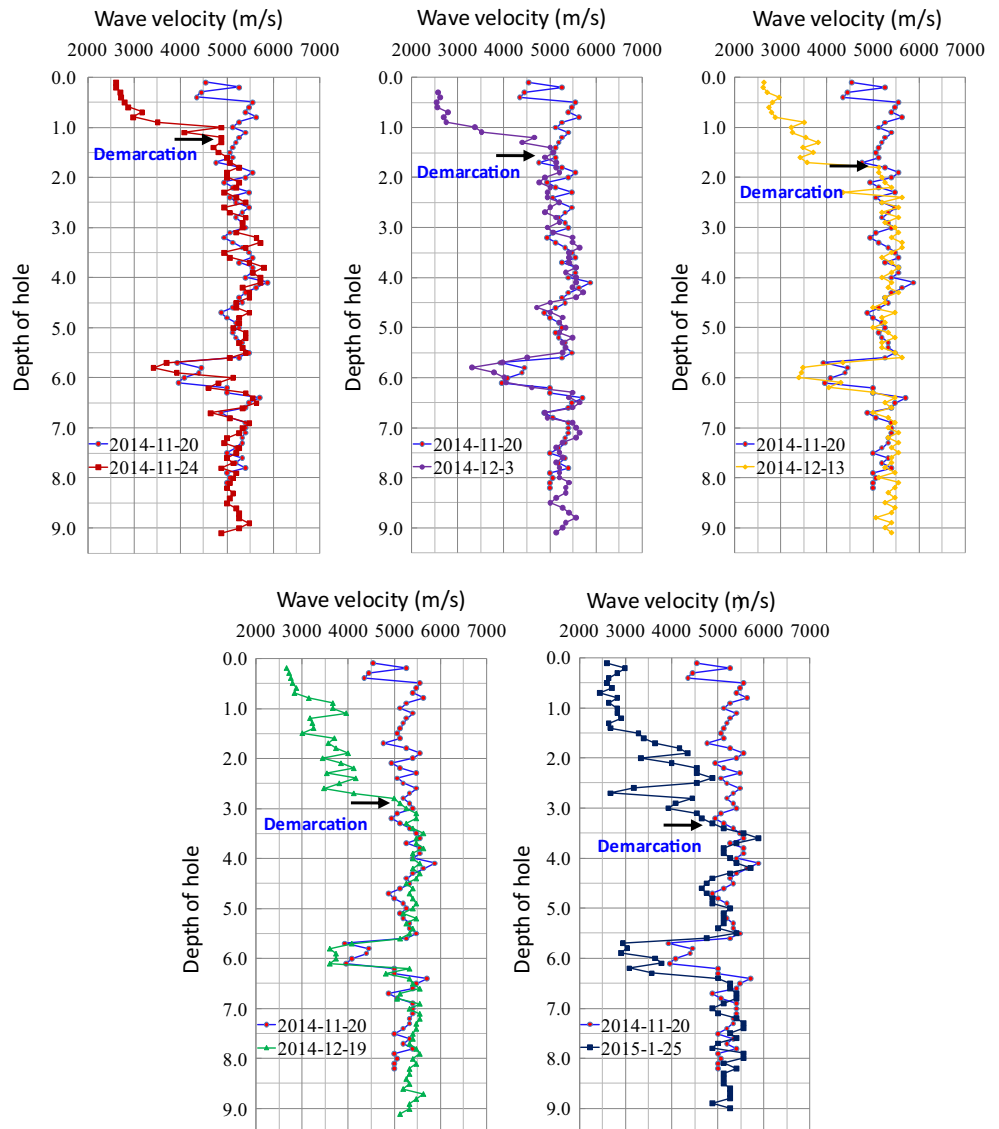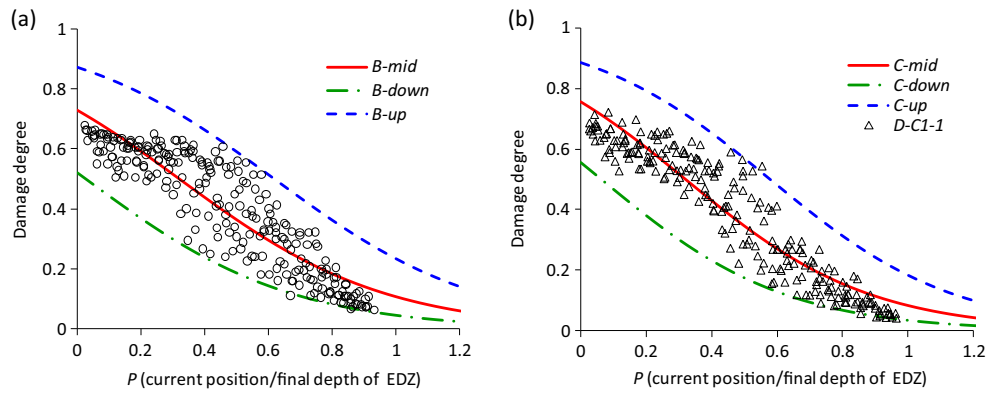
Fig. 17 Regression analysis respectively for the damage data of subzone B (**a**) and subzone C (**b**)

Conclusions

The columnar jointed rock mass is a special geo-material with its natural self-organized network normally in a hexagonal prismatic shape. However, in situ investigations of the CJB on the Baihetan dam foundation showed that most of the transverse sections were quadrangular and pentagonal, and a few were trilateral and hexagonal. The edge lengths were in a
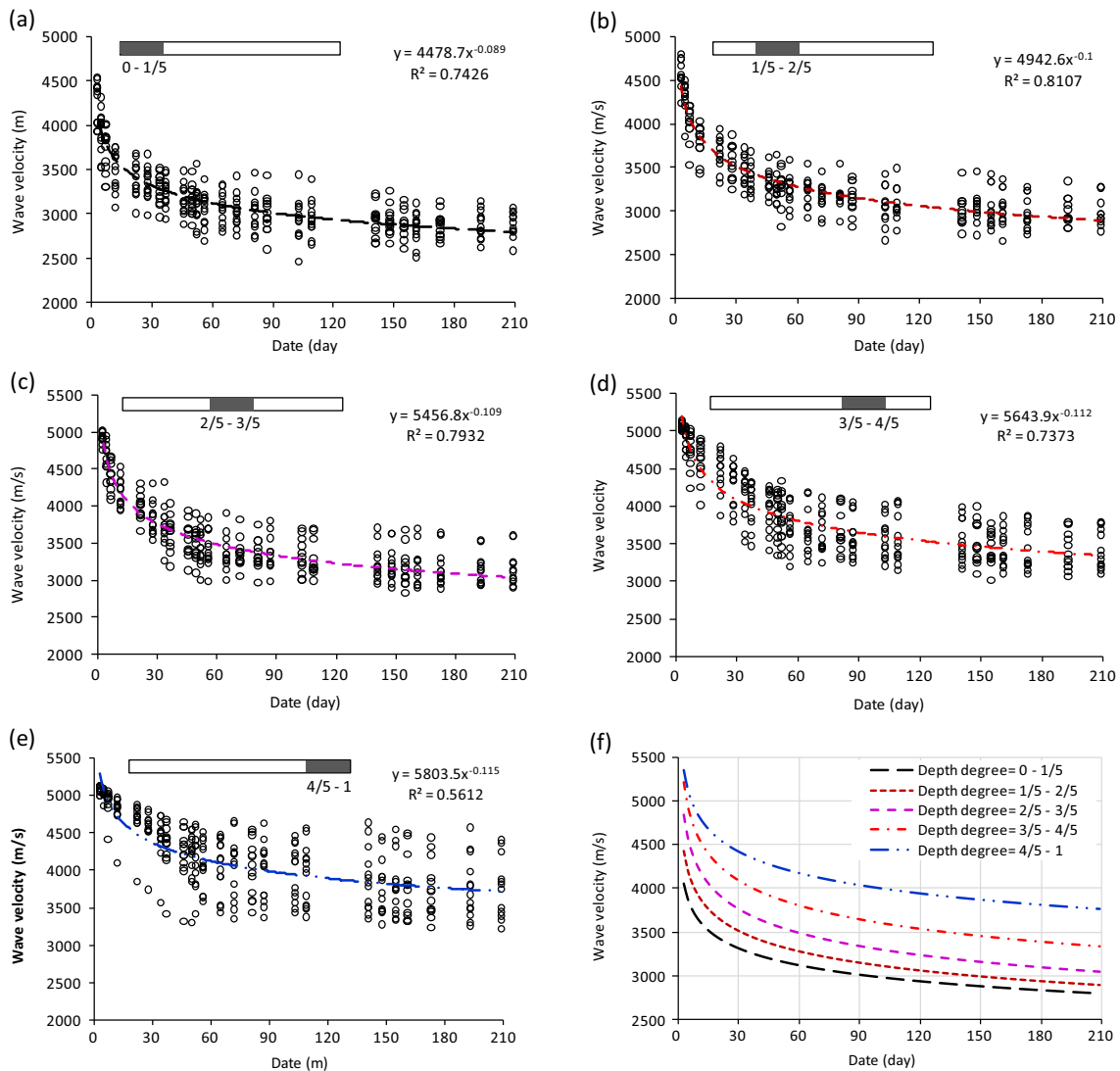

Fig. 18 Time-dependent evolution of the CJB P wave velocity at different depth and corresponding fitting curves in the EDZ: (**a**) 0–1/5 EDZ depth, (**b**) 1/5–2/5 EDZ depth, (**c**) 2/5–3/5 EDZ depth, (**d**) 3/5–4/5 EDZ depth, (**e**) 4/5–1 EDZ depth
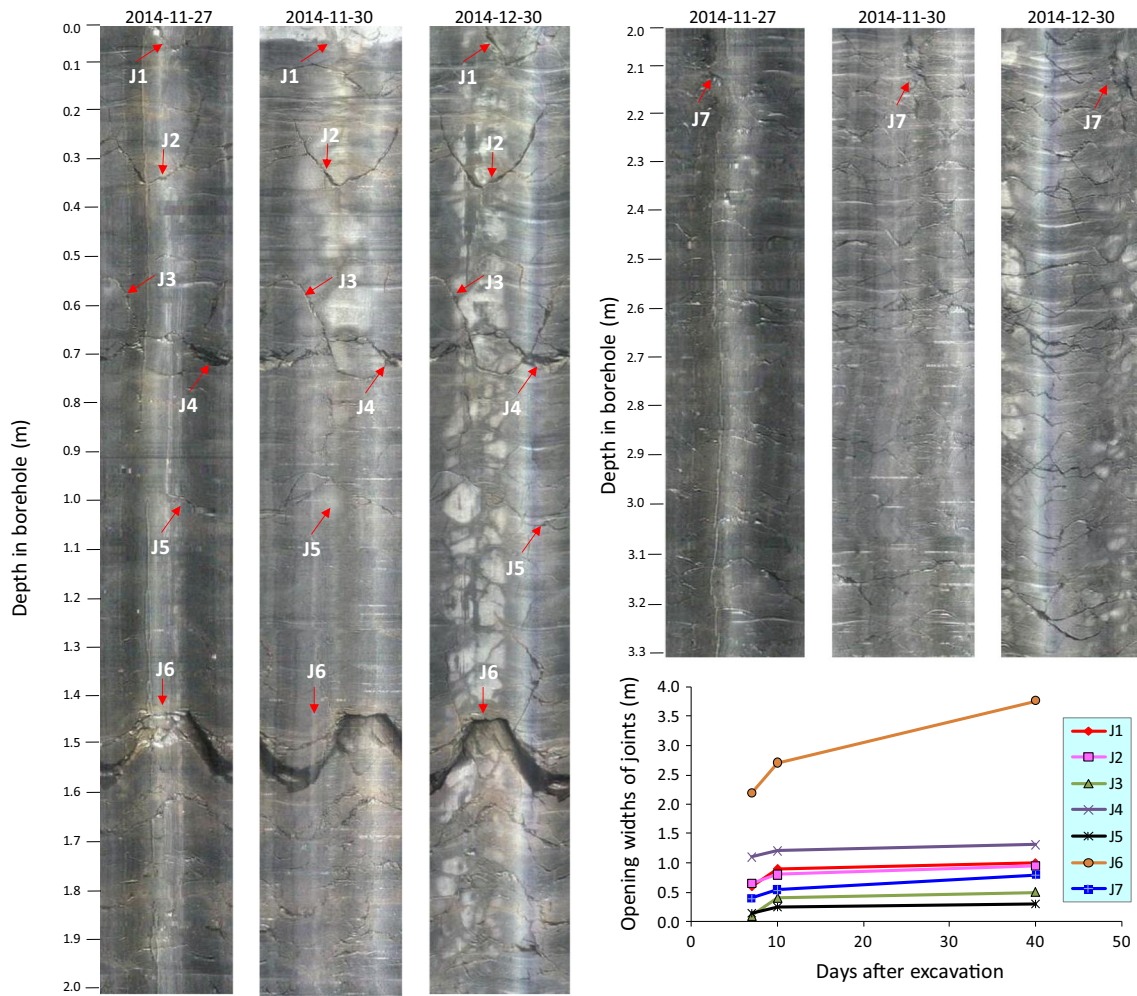
Fig. 19 Time-dependent cracking development of the borehole jointed rock mass observed by digital borehole camera

logarithmic normal distribution instead of being uniformly distributed, with a mean length of 29 cm. The joint network inside the CJB included not only the columnar joints but also the horizontally and vertically distributed internal joints with different historical origins and mechanical properties.

Field ultrasonic P wave tests for the damaged columnar jointed rock mass revealed that the Baihetan CJB had a specific time-dependent damage property. By using backward regression analysis, it was shown that: (1) the EDZ depth increased with time after excavation and converges in a certain
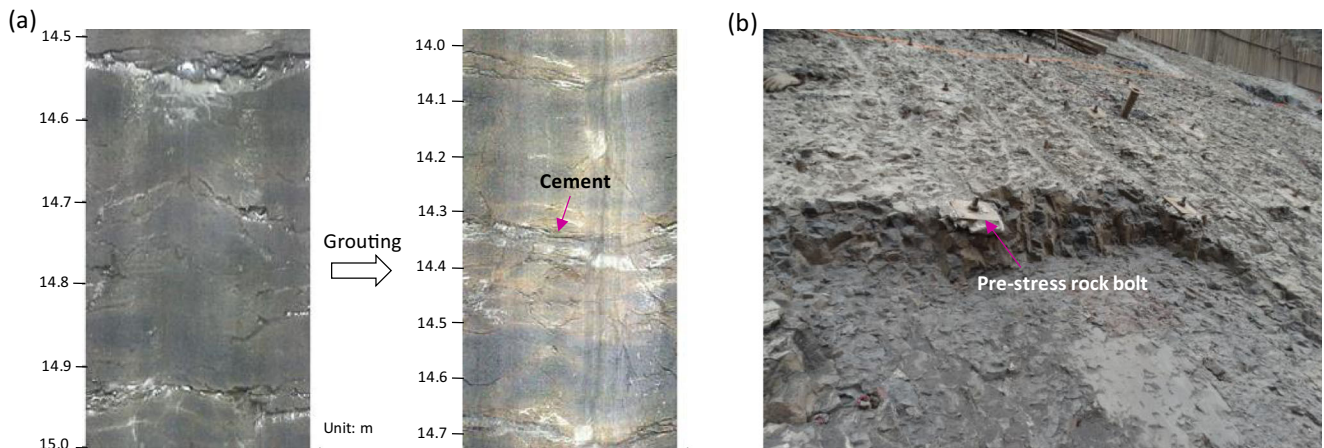

Fig. 20 Actual reinforcement for the jointed basalt: (a) grouted cement observed by digital borehole camera; (b) pre-stress rock bolt on the dam foundation

time depending on the rock quality, which was in accordance with the Curtis logic equation; (2) the CJB damage degree in the EDZ varied in position in accordance with the Sigmoid function; and (3) the EDZ damage degree also changed with time, and its wave velocity fitted a negative exponential function. Overall, the damage evolution of the CJB's EDZ on the Baihetan dam foundation can be considered as a 4D process, i.e., spatially inhomogeneous distribution and time-dependent evolution.

Successive field observations using a digital borehole camera indicated that the unloading damage mechanism of the Baihetan CJB was mainly related to the time-dependent opening of the initially blank and closed joints after excavation. For improving the mechanical properties of the damaged CJB, two reinforcing methods, i.e., the injection of liquid cement and the installation of prestressed rock bolts inside this damaged rock mass, have been suggested.

References

Armand G, Leveau F, Nussbaum C, Vaissiere RDL, Noiret A (2014) Geometry and properties of the excavation-induced fractures at the Meuse/haute-Marne URL drifts. Rock Mech Rock Eng 47(1):21–41

Aydin A (2014) Upgraded ISRM suggested method for determining sound velocity by ultrasonic pulse transmission technique. Rock Mech Rock Eng 47(1):255–259

Brady BHG, Brown ET (1985) Rock mechanics for underground mining. Springer, Dordrecht

Bonilla-Sierra V, Scholtes L, Donze FV, Elmouttie MK (2015) Rock slope stability analysis using photogrammetric data and DFN–DEM modelling. Acta Geotech 10(4):497–511

Budkewitsch P, Robin PY (1994) Modelling the evolution of columnar joints. J Volcanol Geotherm Res 59(3):219–239

Bosshard SA, Mattsson HB, Hetényi G (2012) Origin of internal flow structures in columnar-jointed basalt from Hrepphólar, Iceland: I. textural and geochemical characterization. Bull Volcanol 74(7): 1645–1666

Barton N, Lien R, Lunde J (1974) Engineering classification of rock masses for the design of tunnel support. Rock Mech Rock Eng 6: 189–236

Chen X, Xu Z (2017) The ultrasonic P-wave velocity-stress relationship of rocks and its application. Bull Eng Geol Environ 76: 661–669

Cui J, Jiang Q, Feng XT et al (2018) Insights into statistical structural characteristics and deformation properties of columnar jointed basalts: field investigation in the Baihetan dam base, China. Bull Eng Geol Environ 77(2):775–790

El-Naqa A, Kuisi MA (2002) Engineering geological characterisation of the rock masses at Tannur dam site. South Jordan Environ Geol 42(7):817–826

Fahimifar A, Soroush H (2005) Effect of time on the stress–strain behaviour of a single rock joint. Bull Eng Geol Env 64(4):383–396

Fan QX, Zhou SX, Yang N (2015) Optimization design of foundation excavation for Xiluodu super-high arch dam in China. J Rock Mech Geotech Eng 7(2):120–135

Fang SM, Li JF, Wu SL (2011) Large six-party columnar joints of acidic volcanic rocks and its geological causes and significance in Hong Kong China. Mar Sci 35(5):89–94

Feng XT, Hao XJ, Jiang Q et al (2016) Rock cracking indices for improved tunnel support design: a case study for columnar jointed rock masses. Rock Mech Rock Eng 49(6):2115–2130

Gage JR, Wang HF, Fratt D, Turner AL (2014) In situ measurements of frock mass deformability using fiber Bragg grating strain gauges. Int J Rock Mech Min Sci 71(71):350–361

Goehring L, Lin Z, Morris SW (2006) An experimental investigation of the scaling of columnar joints. Phys Rev E 74(036115):1–13

GB 50218 (1995) Standard for engineering classification of rock mass. Ministry of Water Resources of the People's Republic of China, Beijing

Hetenyi G, Taisne B, Fanny G et al (2012) Scales of columnar jointing in igneous rocks: field measurements and controlling factors. Bull Volcanol 74(2):457–482

Hoek E, Brown ET (1997) Practical estimates of rock mass strength. Int J Rock Mech Min Sci 34:1165–1186

Justo JL, Garcıa-Nunez JC, Vazquez-Boza M, Justo E, Durand P (2014) Design of Raft Foundations for high-rise buildings on jointed rock. Rock Mech Rock Eng 47(4):1277–1290

Jin CY, Yang CX, Fang D, Xu S (2015) Study on the failure mechanism of basalts with columnar joints in the unloading process on the basis of an experimental cavity. Rock Mech Rock Eng 48(3):1275–1288

Jiang Q, Feng XT, Hatzor YH et al (2014) Mechanical anisotropy of columnar jointed basalts: an example from the Baihetan hydropower station, China. Eng Geol 175(3):35–45

Justo JL, Justo E, Durand P et al (2006) The Foundation of a 40-storey tower in jointed basalt. Int J Rock Mech Min Sci 43(2):267–281

Kofichko AV (1996) Characteristics of deformation of the rock mass in the foundation of high concrete dams. Hydrotech Constr 30(8):445–449

Kachanov LM (1958) Time of the rupture process under creep conditions. Izv.akad. Nauk. SSSR Otd Tech Nauk: 26–31

Li JL, Wang LH, Wang XX, Wang RH, Cheng Z, Dang L (2010) Research on unloading nonlinear mechanical characteristics of jointed rock masses. J Rock Mech Geotech Eng 2(4):357–364

Li SJ, Feng XT, Wang CY, Hudson JA (2013) ISRM suggested method for rock fractures observations using a borehole digital optical Televiewer. Rock Mech Rock Eng 46(3):635–644

Li SJ, Feng XT, Li ZH et al (2011) In situ experiments on width and evolution characteristics of excavation damaged zone in deeply buried tunnels. Sci Chin S E Tech Sci 54(s1):167–174

Lin P, Zhou WY, Liu H (2015) Experimental study on cracking, reinforcement, and overall stability of the Xiaowan super-high arch dam. Rock Mech Rock Eng 48(2):819–841

Lore J, Gao H, Aydin A (2000) Viscoelastic thermal stress in cooling basalt flows. J Geophys Res 105(B10):23695–23709

Lucas G, Stephen WM (2008) Scaling of columnar joints in basalt. J Geophys Res 113(B10203):1–18

Luo D, Lin P, Li QB, Zheng D, Lin H (2015) Effect of the impounding process on the overall stability of a high arch dam: a case study of the Xiluodu dam. Chin Arab J Geosci 8(11):9023–9041

Maxwell SC, Young RP, Read RS (1998) A micro-velocity tool to assess the excavation damaged zone. Int J Rock Mech Min Sci 35:235–247

Millard A, Jobst M, Amel R, Uehara S (2009) Study of the initiation and propagation of excavation damaged zones around openings in argillaceous rock. Environ Geol 57(6):1325–1335

Maleki MR (2011) Study of the engineering geological problems of the Havasan dam, with emphasis on clay-filled joints in the right abutment. Rock Mech Rock Eng 44(6):695–710

Malan DF (2002) Simulating the time-dependent behaviour of excavations in hard rock. Rock Mech Rock Eng 35:225–254

Müller G (1998) Starch columns: analog model for basalt columns. J Geophys Res 103(B7):15239–15253

Meglis IL, Chow T, Martin CD, Young RP (2005) Assessing in situ microcrack damage using ultrasonic velocity tomography. Int J Rock Mech Min Sci 42(1):25–34

Malmgren L, Saiang D, Toyra J et al (2007) The excavation disturbed zone (EDZ) at Kiirunavaara mine, Sweden—by seismic measurements. J Appl Geophys 61:1–15

Nabil SA, Ala D (2001) Geological and geotechnical characteristics of Karameh dam site, north of the Dead Sea, Jordan. Bull Eng Geol Environ 60(4):291–299

Ozcan NT, Ulusay R, Isik NS (2013) A study on geotechnical characterization and stability of downstream slope of a tailings dam to improve its storage capacity (Turkey). Environ Earth Sci 69(9):1871–1890

Pei JL, Fei WP, Liu JF (2016) Spatial evolution and fractal characteristics of natural fractures in marbles under uniaxial compression loading based on the source location technology of acoustic emission. Environ Earth Sci 75(9):828–836

PSCC (The Professional standards compilation group of China) (2003) SL282–2003 design specification for concrete arch dams. China Water Power Press, Beijing

PSCC (The Professional standards compilation group of China) (2005) SL319–2005 design specification for concrete gravity dams. China Water Power Press, Beijing

Rodriguez RF, Nicieza CG, Gayarre FL, Herrera EA (2014) Characterization of intensely jointed rock masses by means of in situ penetration tests. Int J Rock Mech Min Sci 72:92–99

Rabtonov N (1963) Progress in applied mechanics. Macmillan, New York, pp 307–315

Sharifzadeh M, Sharifi M, Delbari SM (2010) Back analysis of an excavated slope failure in highly fractured rock mass: the case study of Kargar slope failure (Iran). Environ Earth Sci 60(1):183–192

Satıcıo O, Unver B (2015) Assessment of tunnel portal stability at jointed rock mass: a comparative case study. Comput Geotech 64:72–82

Scholtès L, Donzé F (2015) A DEM analysis of step-path failure in jointed rock slopes. C R Mecanique 343(2):155–165

Shao JF, Chauc KT, Feng XT (2006) Modeling of anisotropic damage and creep deformation in brittle rocks. Int J Rock Mech Min Sci 43(4):582–592

Schultz RA (1995) Limits on strength and deformation properties of jointed basaltic rock masses. Rock Mech Rock Eng 28(1):1–15

Shan ZG, Di SJ (2013) Loading-unloading test analysis of anisotropic columnar jointed basalts. J Zhejiang Univ Sci A 14(8):603–614

Shi AC, Tang MF, Zhou Q (2008) Research of deformation characteristics of columnar jointed basalt at Baihetan hydropower station on Jinsha river. Chin J Rock Mech Eng 27(10):2079–2086 (in Chinese)

Sakurai S (2010) Modeling strategy for jointed rock masses reinforced by rock bolts in tunneling practice. Acta Geotech 5:121–126

Saliba R, Jagla EA (2003) Analysis of columnar joint patterns from three-dimensional stress modeling. J Geophys Res 108(B10):1–7

Weinberger R, Eyal Y, Mortimer N (2010) Formation of systematic joints in metamorphic rocks due to release of residual elastic strain energy, Otago schist, New Zealand. J Struct Geol 32(3):288–305

Watters RJ, Zimbelman DR, Bowman SD, Crowley JK (2000) Rock mass strength assessment and significance to edifice stability, Mount Rainier and Mount Hood Cascade Range Volcanoes. Pure Appl Geophys 157(6–8):957–976

Wu ZR, Gu YC, Su HZ, Guo HQ (2009a) Mechanical effects of excavation rebound of arch dam bedrock and better concreting time of dam body. Sci Chin S E Tech Sci 52(2):513–517

Wu FQ, Liu JY, Tong L, Zhuang H, Yan C (2009b) A method for assessment of excavation damaged zone (EDZ) of a rock mass and its application to a dam foundation case. Eng Geol 104(3):254–262

Xiang Y, Wang L, Wu SH, Yuan H, Wang Z (2015) Seepage analysis of the fractured rock mass in the foundation of the main dam of the Xiaolangdi water control project. Environ Earth Sci 74(5):4453–4468

Xu WY, Zheng WT, Shi AC (2011) Classification and quality assessment of irregular columnar jointed basaltic rock mass for hydraulic engineering. J Hydraul Eng 42(3):262–270 (in Chinese)

Yarahmadi R, Bagherpour R, Sousa LO, Taherian SG (2015) How to determine the appropriate methods to identify the geometry of in situ rock blocks in dimension stones. Environ Earth Sci 74(9):6779–6790

Yan DX, Xu WY, Zheng WT et al (2011) Mechanical characteristics of columnar jointed rock at dam base of Baihetan hydropower station. J Cent S Univ Technol 18(6):2157–2162 (in Chinese)

Zhu WS, Chen YJ, Li SC, Yin FQ, Yu S, Li Y (2014) Rock failure and its jointed surrounding rocks: a multi-scale grid meshing method for DDARF. Tunn Undergr Space Technol 43(7):370–376

Zhang ZP, Zhang R, Xie HP, Liu J, Were P (2015) Differences in the acoustic emission characteristics of rock salt compared with granite and marble during the damage evolution process. Environ Earth Sci 73(11):6987–6999

Zhan SS, Wang TT, Huang TH (2016) Variations of hydraulic conductivity of fracture sets and fractured rock mass with test scale: case study at Heshe well site in Central Taiwan. Eng Geol 206:94–106

Zhang W, Zhao Q, Huang RQ et al (2016) Identification of structural domains considering the size effect of rock mass discontinuities. A case study of an underground excavation in Baihetan dam. China Tunn Undergr Space Technol 51:75–83